Partial optimization of molecular geometry in normal coordinates and use as a tool for simulation of vibrational spectra

Petr Bouř[a)]
Institute of Organic Chemistry and Biochemistry, Academy of Sciences of the Czech Republic, Flemingovo nám. 2, 16610, Praha 6, Czech Republic

Timothy A. Keiderling
Department of Chemistry (M/C 111), University of Illinois at Chicago, Chicago, Illinois 60607-7061

A normal mode coordinate-based molecular optimization algorithm was implemented and its performance tested against other optimization techniques. In certain cases the method was found to be computationally simpler and numerically more stable than the optimization algorithms based on Cartesian or internal valence coordinates. The usual redundant/internal coordinate scheme provided fastest convergence for compact covalently bonded molecules, while the normal mode method was found to be more suitable for more weakly bonded molecular complexes. For constrained optimizations use of the normal coordinates allows one to naturally separate the lower-energy modes from those more typically studied with vibrational spectroscopy. Thus, it provides an appropriate tool for simulations of IR and Raman spectra of larger molecules and complex systems when specific conformations are desired. © *2002 American Institute of Physics.*
[DOI: 10.1063/1.1498468]

I. INTRODUCTION

In the theoretical modeling, molecular motion is often arbitrarily restricted. For example, in order to calculate vibrational spectra of biologically interesting systems, natural structures often have to be simplified and thus accessible to advanced computations. This can cause problems since the desired conformations can significantly deviate from relaxed geometries obtained within a given approximation. In other words, formal full energy minimization is not relevant in such cases. Traditionally, constrained optimization techniques are applied separating out geometry parameters (e.g., torsion angles) that should have little influence on desired molecular properties (e.g., mid-IR vibrational frequencies). In this work, a normal mode following technique is proposed as a computationally more convenient alternative to the valence-coordinate constraints.

Optimization of molecular structure by energy minimization has always been a focus of computational chemistry. A rather restricted class of algorithms has been found relevant to *ab initio* quantum-mechanical computations, because of their exceptional demands on computer power. Methods based on a quadratic approximation of the molecular potential energy surface appear to be most convenient,[1] although particular advantages can be found also for other approaches, such as those using a conjugate gradient[2,3] or the direct inversion of the iterative subspace.[4,5] For the quadratic methods, the molecular Hessian, i.e., the matrix of the energy second derivatives (force constants), is estimated either in each optimization step or by updating on the fly. Updating is usually preferred, because for most *ab initio* methods computation of the gradient takes a small fraction of the time needed for evaluation of a complete Hessian. Of the many available updating schemes, the Davidon–Fletcher–Powell,[6] Schlegel,[1] and Broyden–Fletcher–Goldfarb–Shanno (BFGS)[7] algorithms have proven to be most successful for molecular studies. The assumption of a quadratic potential enables use of the Newton–Raphson or semi-Newton–Raphson (scaled) gradient optimization scheme. However, it was realized early that this scheme must be generalized for more general molecular surfaces farther from the quadratic region. Thus, the trust radius model[8] derives the step size from Hessian eigenvalues, while the more universal rational function optimization (RFO)[9,10] method introduces a self-consistent, self-controlled step scaling optimization.

The choice of a suitable coordinate system, normally a trivial linear transformation, is of paramount importance for molecular optimizations. Quantum chemical programs usually provide gradients and Hessians in Cartesian coordinates, which are not suitable for most molecular optimizations. However, it was shown that for many molecules, particularly for cyclic systems, optimization in Cartesian coordinates is numerically more stable and often converges faster than methods based on internal coordinates.[11] Consequently, methods based on mixed internal and Cartesian coordinates were proposed and proved to be a viable alternative.[12,13] Pulay and co-workers, however, showed that the problems associated with valence-type coordinate optimizations can be overcome by an introduction of carefully chosen natural or, most conveniently, redundant internal coordinates.[14,15]

In our experience, however, redundant coordinates are not always the best choice. Optimization of large molecules

---
[a)]Author to whom correspondence should be addressed. Electronic mail: bour@uochb.cas.cz

J. Chem. Phys., Vol. 117, No. 9, 1 September 2002

Optimization of molecular geometry   4127

using the GAUSSIAN set of programs[16] (where the redundant algorithm is implemented) often did not converge successfully, presumably because of the numerical instabilities generated by the large number of matrix–matrix multiplications needed for back and forth Cartesian/redundant transformations. A recent study suggested that the numerical stability should be improved using an approximate Cholesky factorization technique.[17] More complex constrained optimizations are often limited; for example, when constraints involve linear combinations of the internal coordinates, they cannot be held fixed except by special techniques, such as Lagrangian multipliers, the projector method, or the penalty-function approach.[1]

In the past, we used constrained optimization based on internal (nonredundant or redundant) coordinates, namely for torsion angles, in order to obtain peptide fragments with specifically defined conformations, but otherwise geometrically fully relaxed so that the spectroscopically important higher frequency modes were not significantly perturbed.[18,19] Apart from the difficulties described above, such procedure proved to be unstable namely for weakly bonded molecular complexes with noncovalent interactions, such as DNA base pairs or solvent–solute complexes. An automatic definition of the redundant coordinates is not often desirable and user intervention is required for these systems, optimally involving a manual inspection or redefinition of all the noncovalent geometry parameters. Furthermore, it is not *a priori* clear which vibrational modes are affected by fixing specific internal coordinates. Thus, we propose instead a normal mode based optimization that, as shown below, more elegantly balances the conflicting goals of fixing geometry parameters and relaxing the vibrational degrees of freedom.

Normal mode (eigenvalue) following algorithms have previously proven to be indispensable for transition state localization. General algorithms allowing separation of the vibrational modes have been proposed for geometry optimizations as well as for finding energy maxima or higher-order saddle points.[20–23] This existing mathematical apparatus can thus be readily adapted for constraining or relaxing a normal mode coordinate. In the next sections we describe our implementation of the normal mode optimization method and, through several examples, compare it to the more usual molecular optimization techniques.

II. METHOD

A. The harmonic approximation

We introduce the harmonic approximation[24] in order to define basic variables used for the normal mode optimization algorithm. The molecular harmonic vibrational Hamiltonian is given by

$$H = \tfrac{1}{2}(\Delta \dot{\mathbf{x}}^t \cdot \mathbf{M} \cdot \Delta \dot{\mathbf{x}} + \Delta \mathbf{x}^t \cdot \mathbf{f} \cdot \Delta \mathbf{x}), \qquad (1)$$

where $\mathbf{M}$ is diagonal matrix of atomic masses $\{m_i\}$, $\Delta \mathbf{x}$ is the vector of atomic displacements with respect to their equilibrium positions, $\Delta x_i = x_i - x_i^0$, and $\mathbf{f}$ is the Cartesian force constant matrix (Hessian). Bold letters denote vectors or matrices, superscript ^{t} means transpose. Following common practice, the index $(i = 1,...,3N)$ consists of the atom number
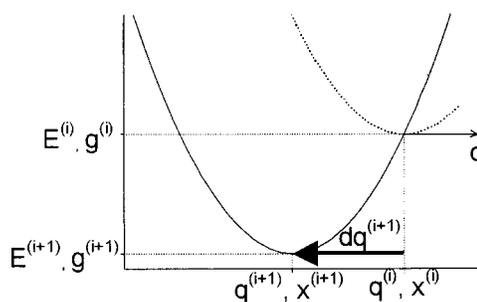
FIG. 1. Normal mode optimization. At each point i a quadratic potential energy surface is assumed to be same as at the final/next point $i+1$. Note, that normal mode displacement dq_i has a different sign if related to the parabolas at i and $i+1$.

$(\lambda = 1,...,N)$ and a coordinate $(\alpha = x,y,z)$. As an intermediate step, mass-weighted coordinates are defined so that $X_i = \sqrt{m_i}\,\Delta x_i$, $f_{ij} = \sqrt{m_i m_j}\,F_{ij}$, and

$$H = \tfrac{1}{2}(\dot{\mathbf{X}}^t \cdot \dot{\mathbf{X}} + \mathbf{X}^t \cdot \mathbf{F} \cdot \mathbf{X}). \qquad (2)$$

Finally, introducing the normal mode coordinates, $\{q_j\}$,

$$\mathbf{X} = \mathbf{s} \cdot \mathbf{q},$$

and requiring

$$\mathbf{s}^t \cdot \mathbf{s} = \mathbf{1}, \quad \mathbf{s}^t \cdot \mathbf{F} \cdot \mathbf{s} = \mathbf{Q}, \quad \text{with} \quad Q_{ij} = \omega_i^2 \delta_{ij},$$

we obtain the Hamiltonian in a diagonal form as a sum of harmonic oscillators

$$H = \tfrac{1}{2}(\dot{\mathbf{q}}^t \cdot \dot{\mathbf{q}} + \mathbf{q}^t \cdot \mathbf{Q} \cdot \mathbf{q}) = \sum_j \tfrac{1}{2}(\dot{q}_j^2 + \omega_j^2 q_j^2). \qquad (3)$$

The Cartesian displacements are thus related to the normal mode coordinates via a linear transformation

$$\Delta x_i = \sum_j \frac{1}{\sqrt{m_i}} s_{ij} q_j = \sum_j S_{ij} q_j, \qquad (4)$$

i.e., with the well-known $\mathbf{S}$-matrix transformation.

B. The normal mode optimization

The usual quadratic approximation (Fig. 1) is used to search for the energy minimum. Knowing the normal mode gradient, $\mathbf{g^{(i)}}$, and the second derivatives of the energy, $\mathbf{Q^{(i)}}$, at an optimization point i, the step towards the minimum energy is given by the Newton–Raphson formula modified according to the RFO[9,10] method. In a pseudocode representation, the present algorithm follows these steps.

(1) Estimation of initial $\mathbf{f^{(i)}}$, yielding the $\mathbf{S}$ matrix.
(2) Calculation of the Cartesian gradient $\mathbf{g_c^{(i)}}$.
(3) If a previous step is available, update $\mathbf{f}$ using the BFGS Hessian update[7]

$$\mathbf{f}^{(i+1)} = \mathbf{f}^{(i)} - \left(\frac{\Delta \mathbf{g}^{(i)t} \Delta \mathbf{g}^{(i)}}{\mathbf{dx}^{(i)} \cdot \Delta \mathbf{g}^{(i)}} + \frac{(\mathbf{f}^{(i)} \cdot \mathbf{dx}^{(i)})^t \mathbf{dx}^{(i)} \cdot \mathbf{f}^{(i)}}{\mathbf{dx}^{(i)} \cdot \mathbf{f}^{(i)} \cdot \mathbf{dx}^{(i)}} \right), \qquad (5)$$

with Cartesian displacements $\mathbf{dx}^{(i)} = \mathbf{x}^{(i)} - \mathbf{x}^{(i-1)}$ and the gradient differences $\Delta \mathbf{g}^{(i)} = \mathbf{g_c}^{(i)} - \mathbf{g_c}^{(i-1)}$. Obtain new $\mathbf{S}$-matrix.

(4) Calculate the normal mode gradient

$$\mathbf{g}^{(i)} = \mathbf{S}^t \cdot \mathbf{g}_c^{(i)}. \tag{6}$$

If small, stop the optimization.

(5) Produce a new step, using the quadratic dependence and its RFO[1,9–11,13] extension

$$\mathbf{dq}^{(i+1)} = -\frac{2\mathbf{g}^{(i)}}{\mathbf{Q}_{ii} + \sqrt{\mathbf{Q}_{ii}^2 + 4(\mathbf{g}^{(i)})^2}}. \tag{7}$$

(6) Produce new Cartesian coordinates

$$\mathbf{x}^{(i+1)} = \mathbf{x}^{(i)} - \mathbf{S} \cdot \mathbf{dq}^{(i+1)}. \tag{8}$$

(7) Increment i, and iterate back to step 2.

C. Implementation

The normal mode optimization was implemented in a driving program QGRAD, which reads energies, gradients, and second derivatives from an *ab initio* output, and produces improved coordinates. Also, the normal mode calculation (force-field diagonalization) and the coordinate transformations (see steps 1–7 above) are controlled by QGRAD. Currently, the program is interfaced to the GAUSSIAN program package.

The optimizations in Cartesian and internal/redundant coordinates were done with GAUSSIAN using the default Berny[25] optimization routes and the common *ab initio* methods specified below for each particular system.

III. RESULTS

A. Azetidine full optimization

In order to investigate the general properties of this normal modes-based optimization, the azetidine molecule
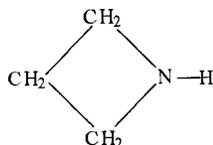
was chosen, since it was originally used as a test for the redundant coordinate method.[14] The starting geometry was obtained with the TINKER[26] molecular mechanics package and was further optimized at the HF/4-31G level. The convergence was determined on the basis of the mean Cartesian ($< \sim 10^{-5}$ a.u.) or corresponding normal mode gradient corresponding approximately to an energy error of 10^{-7} hartree.

As follows from the dependence of energies (in logarithmic scale) on the step number in Fig. 2, Cartesian coordinates provided a steady convergence but needed about 36 steps for a complete optimization. The internal (nonredundant) valence coordinates provided an apparent fast energy decrease at the beginning, but the convergence stopped approximately at the step number 20 and the energy error kept oscillating within a small energy interval (10^{-3} hartree ~ 1 kcal/mol). The redundant coordinate method converged smoothly after 13 steps. The normal mode optimization provided the faster convergence at the beginning, but was finished later, in about 18 steps. Thus, the redundant coordinate
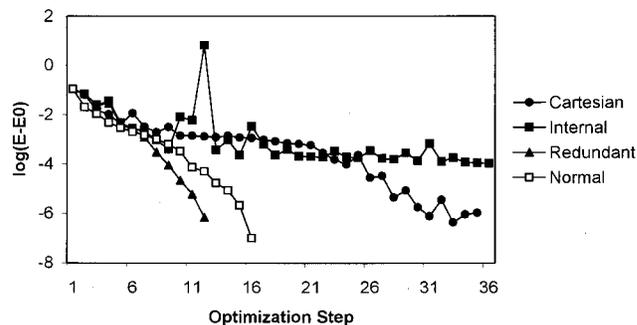
FIG. 2. Azetidine HF/4-31G full optimization. The dependence of the energy error on the number of optimization steps for the four coordinate systems.

method proved to be most advantageous for azetidine, in accord with its reputation,[15,17] but the normal mode method seems to be a reasonable alternative, still much faster than the Cartesian-based optimization. We have observed this property of the normal mode method (slightly slower than the redundant, but much faster than the Cartesian) for most other molecules that were optimized without constraints.

Interestingly, the curves for the three converging methods (Cartesian, redundant, normal) in Fig. 2 exhibit an "S" pattern, with the fastest energy decreases at the beginnings and at the ends of the optimization paths. This presumably reflects the large geometry changes for the first optimization points as well as the approach to the quadratic potential energy surface at the final stages of the optimization.

B. Oligopeptide torsion angles

The conformation of peptides and proteins is essential for their biological activity and other physical properties, and has been the topic of numerous spectroscopic studies. In the next example the normal mode method is used to constrain the geometry during the optimization. Unlike for the valence coordinate optimizations, the peptide main chain torsion angles (ϕ, ψ) are not fixed explicitly. Rather, the low-frequency modes involving these torsions are frozen.

Similar to the methods used in Ref. 17, a tripeptide molecule, Ac-(Ala)$_3$NHMe, was generated in a β-sheet-like extended conformation $[(\psi, \phi) = (135°, -135°)]$ by the TINKER program package. Then, constrained optimizations were performed at the HF/6-31G level, using the internal/redundant method with fixed (ϕ, ψ), and the normal mode optimization with limits on the maximum frequencies of the fixed modes. We suppose that the results can be generalized to any other computational model; the HF/6-31G level was chosen in order to save computational time. Although calculated frequencies deviate from expected experimental values, generally being too high by 10%–15%, it has been established that reasonable estimates of experimental frequencies can be obtained with this level if a simple scaling of computed numbers is allowed.[27]

The torsion angle changes are summarized in Table I for the C-terminal residue only, since they do not vary significantly and virtually the same numbers were obtained for the other two alanine residues. Apparently, fixing of the lower-

TABLE I. The oligopeptide Ac-(Ala)$_3$NHMe HF/6-31G constrained optimization.

	Torsion angles (ψ,ϕ)[a]	Energy (a.u.)	Number of steps	$\omega_I(cm^{-1})$[b]	$\omega_{II}(cm^{-1})$[c]
Starting geometry:					
	135.0, −135.0	−984.094 367	(0)	1893	1759
Fixed normal modes:					
With $\omega < 100$ cm^{-1}	135.6, −134.0	−984.123 008	10	1814	1700
200 cm^{-1}	135.0, −135.0	−984.122 040	9	1817	1696
400 cm^{-1}	135.0, −135.0	−984.118 583	5	1820	1705
600 cm^{-1}	135.7, −135.7	−984.117 834	6	1821	1712
1000 cm^{-1}	134.4, −134.7	−984.116 379	4	1822	1709
Fixed torsions:					
	135.0, −135.0	−984.121 259	4	1816	1701
Unconstrained optimization:					
	162.6, −159.2	−984.129 142	35	1802	1689

[a]For the middle alanine residue; values for other residues were similar within 1°.
[b]The highest C=O stretching (amide I) frequency.
[c]The N–C stretching (amide II) frequency, maximum of absorption.

frequency normal modes effectively does fix the torsional movement, even if the lowest limit is chosen to be 100 cm^{-1}. Indeed, when such a restriction is removed, the molecule relaxes into quite a different conformation with $(\psi,\phi) = (162.6°, -159.2°)$. Optimizing with fixed normal modes provides a molecular energy similar to that obtained with the torsion-angle-based constrained optimization. In the last three columns of Table I characteristic peptide bond frequencies for the amide I (C=O stretching) and amide II (C–N stretching coupled with N–H bending) modes are listed. Clearly, compared with the original structure, both optimizations provide similar improvement in these amide frequencies, with respect to the fully relaxed geometry. For example, the amide II frequency decreased by 77 cm^{-1} during the optimization with fixed torsions, which compares well with the changes (79–71 cm^{-1}) within the fixed normal mode optimizations.

C. Dinucleotide model

Refinement of the DNA geometry from that obtained from via an x-ray structure determination is a typical task required to model its vibrational properties. A particular problem that arises in this process is the preservation of the desired conformation within given computational model for the force field, while still maintaining the normal modes of interest. As an example that models this process, a "dinucle-otide" duplex consisting of two cytosine and guanine pairs was constructed, based on standard B-DNA conformation parameters implemented in the MSI/ACCELRYS software packages. In order to preserve the desired arrangement of the bases, two constrained optimization techniques were applied. First, the normal mode scheme was used, and all normal mode coordinates whose modes had $\omega < 100$ cm^{-1} were held fixed. Then, with the internal coordinate method, the distance between the base pair planes was fixed by creating an arbitrary bond between cytosine and guanine nitrogen atoms, each in the opposite plane, this new bond being approximately perpendicular to the planes. In addition, the bending angles associated with this bond and all molecular torsion angles (involving the hydrogen bonds) were kept constant.

All computations were performed at the BPW91[28,29]/6-31G** level with default GAUSSIAN parameters.

As can be seen from Fig. 3, for this "duplex DNA" model, the normal mode method provided a fast smooth convergence within 23 cycles, while the internal coordinate method had large oscillations in the early stages, then yielded a stabilized structure after approximately 33 steps, but finally began to mildly oscillate in energy, not fully obeying the default convergence criteria in GAUSSIAN. The normal mode optimized energy was ~1 kcal/mol smaller and the rms gradient was 50% smaller than that from the internal coordinate optimization. Both techniques approximately preserved the desired juxtaposition of the bases found in the B-conformation of DNA, as can be judged from Fig. 4, where the starting- and optimized geometries are superimposed. However, the normal mode optimization led to significantly smaller changes of geometry than the internal optimization. For example, the overlap of the starting and internally optimized geometry [case (a) in Fig. 4] produced a root-mean-square (rms) deviation (Δ) of 0.12 Å for 12 atoms in the cytosine six-member rings, while the overlap of the starting- and normal mode optimized geometries resulted in
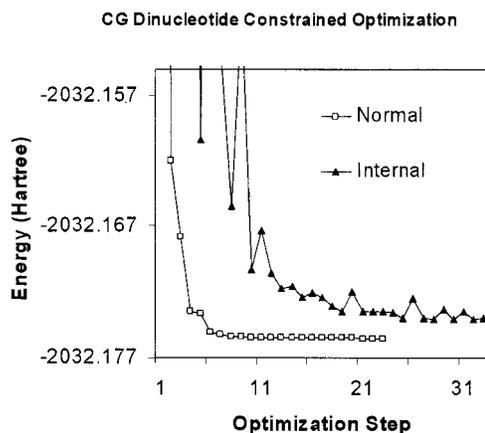
FIG. 3. Progress of the dinucleotide model constrained optimization for the internal and normal mode optimization methods. Both minimizations started from the same original geometry (cf. Fig. 4).

(a)

(b)
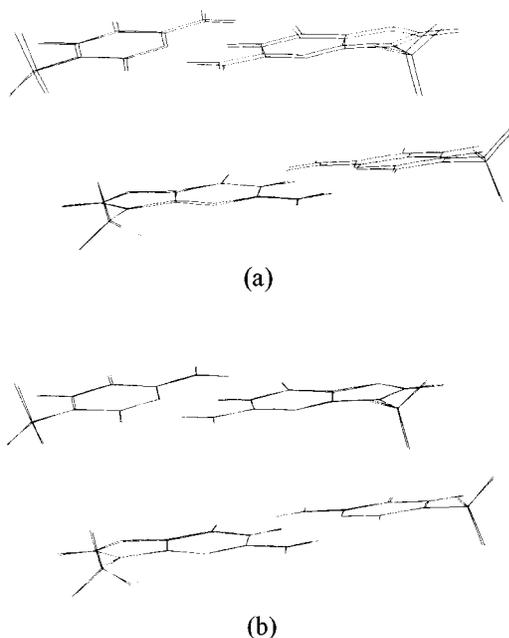
FIG. 4. Superposition of the model dinucleotide starting and final geometries obtained by constraining the internal (a) and normal mode (b) coordinates.

$\Delta = 0.04$ Å. The normal mode constrained optimization thus appears to be more restricted to relaxing the higher-energy small-amplitude movements that are needed in order to find the proper minima for the higher-frequency modes.

In Fig. 5 the simulated IR absorption spectra are plotted, as calculated for the starting geometry and the two optimized geometries of this "dinucleotide." The remarkable similarity of the spectra for the optimized structures and their differences from the original structure spectra suggests that for both optimized cases the modes which are of the most spectroscopic interest, those lying in the region of approximately $1000-2000$ cm^{-1}, are satisfactorily relaxed during the optimization processes. For example, the highest C=O stretching band was calculated to be at a rather unrealistic frequency at 1824 cm^{-1} for the original structure, but moved to
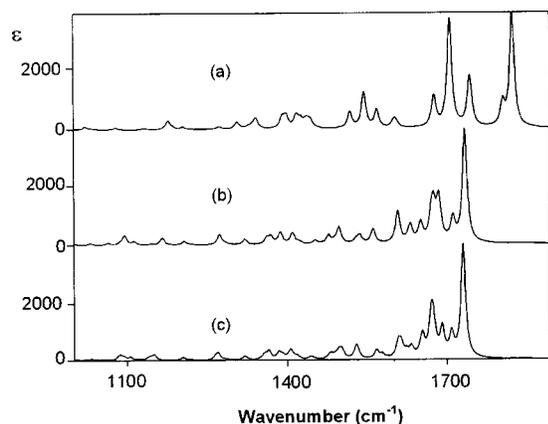
FIG. 5. Dinucleotide duplex IR absorption spectra, as calculated at the BPW91/6-31G** level for the starting geometry (a) and for structures obtained by the constrained normal mode (b) and internal coordinate (c) optimizations.

1734 and 1731 cm^{-1} for the normal mode and internal coordinate optimization, respectively. When the normal frequency errors of this (BPW91/6-31G**) method are taken into account, these compare much better with experimental data measured for such systems.[30] Unfortunately, due to the lack of experimental data for our specific model system we cannot judge which of the two methods provided more realistic IR intensity spectral profile. Nevertheless, we can conclude for the dinucleotide duplex that the normal mode optimization: (1) was found to be numerically more stable; (2) allowed the molecule to be better relaxed (providing lower energy); (3) disturbed the original geometry less, and, finally (4) provided approximately the same vibrational spectra as the classical internal-coordinate-based optimization.

D. Water cluster constrained optimization

Constrained optimizations of systems with ill-defined internal/redundant coordinates, such as might be found in weakly interacting hydrogen-bonded systems, are primary targets of the proposed method. For such systems the automatic redundant/internal routine, as implemented in the GAUSSIAN package, generates non-natural linear-bending coordinates as a substitution for the missing covalent bonds, and these do not provide fast convergence. This can be improved only partially by a user redefinition of those coordinates, which, however, significantly complicates practical computations on these complex systems. In this section we apply the normal mode technique for computations of partially relaxed geometries and vibrational frequencies of a cluster of hydrogen-bonded water molecules and compare the results to the conventional methods.

A cluster of 10 water molecules was prepared as follows using the TINKER program. An approximately cubic water droplet consisting of 214 molecules, constructed using the TINKER example according to the work of Lybrand and colleagues,[31] was minimized using the AMBER[32] force field. Then, a "randomly" selected part consisting of 10 molecules was *ab initio* optimized at the BPW91/6-31G** level. In order to separate the lower-frequency modes and keep the geometry (mutual positions and orientations of the molecules) as close as possible to that found in the droplet, constrained optimizations were performed using: (1) the normal mode method, where coordinates corresponding to modes whose wave number was lower than 100 cm^{-1} were fixed; (2) the redundant coordinate method with all torsion angles fixed; (3) internal coordinates (following the hydrogen bonds) with torsional and bond angles fixed; (4) internal coordinate method with all torsions fixed; and (5) the same as step 3, but covalent H–O–H bond angles were allowed to optimize.

The dependence of the energy on the optimization steps as plotted in Fig. 6 illustrates the very different behavior of these various optimization schemes. Not only did the automatic redundant coordinate method provide no convergence, but it generated geometries with higher energies than the starting structure. The methods based on user-defined internal coordinates (methods 3–5 above) behaved similarly in the early stages of the optimization; consequently, the only successful choice, number 3, is shown in Fig. 6. It provided
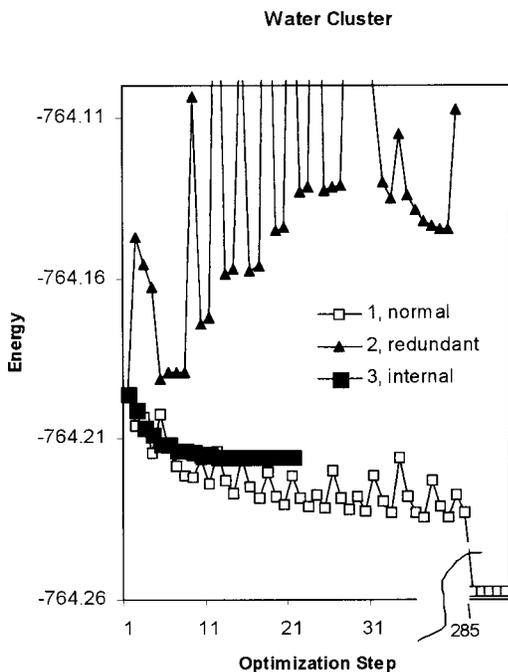
FIG. 6. Progress of the constrained optimizations of the water cluster for the normal mode method (modes with $\omega < 100\ \text{cm}^{-1}$ fixed, number 1 in Table I), for the automatic redundant coordinate procedure (torsion angles fixed, number 2) and for a user-defined internal coordinate set (torsion and bond angles fixed, number 3).

an energy minimum after 21 optimization steps. The normal mode optimization technique converged after a significantly greater number of 288 steps, but also resulted in a much lower value of the total energy.

The overall behavior of the five optimization paths can be compared in detail in Table II. The normal mode optimization (number 1) provided the most relaxed cluster structure, with energy lower by 20–26 kcal/mol than for the structures obtained with the internal coordinate optimization. The degree of relaxation can also be judged from the number of negative (imaginary) vibrational frequencies, reduced by 9 from the 14 for the initial geometry by the normal mode optimization. On the other hand, the internal coordinate optimizations provided about twice as many imaginary frequencies, and these also had much higher absolute values, which presumably means that they may interfere with modes measured in IR spectra. The constrained optimizations based

solely on the torsion angle fixations (optimization 2 and 4) proved to be numerically unstable for this system and did not converge to an energy minimum. Although we do not have immediate experimental data for comparison, we feel that the normal mode optimization is most suitable for this system, enabling a straightforward relaxation of the cluster with controllable treatment of the vibrational properties.

IV. DISCUSSION

There is probably no universal method of optimization suitable for all molecular systems. For most common molecules the redundant coordinate method appears to be the most convenient. For optimizations close to the quadratic region the normal modes can be viewed as a compromise between Cartesian and redundant coordinates, providing faster convergence than the Cartesians and being more numerically stable than the redundant. This can be documented for the example of the azetidine optimization shown in Fig. 2, and is consistent with results of tests for other molecules that we did not include in this work.

The algorithm presented here is computationally simpler than those used for the internal and redundant schemes, avoiding many of the potentially numerically unstable transformation matrix products. The normal modes, unlike internal coordinates, are always exactly related to the Cartesian coordinates by a *linear* transformation [cf. Eq. (4)]. In spite of the simplicity, the continuous Hessian update [Eq. (5)] and the efficient step controlling RFO method [Eq. (7)] could be used, which tremendously accelerates the convergence. Moreover, using the normal mode following RFO step circumvents the iterative search for the λ parameter needed for internal/redundant coordinate sets.[1,7] Finally, since the normal modes are defined exclusively by the force field, minimal effort is required in order to define the best coordinate representation, which makes the method suitable for computer modeling algorithms.

We have tried several other modifications of the normal mode algorithm presented above. For example, a fixed normal mode–Cartesian transformation S-matrix can be defined, based on the original force field, and the (nondiagonal) normal mode Hessian can be updated instead of Eq. (5). These, however, lead to similar results, albeit with slightly more computational demands.

TABLE II. Summary of the outcome of the constrained optimizations of the water cluster using five coordinate sets.

Method	Coordinates	Fixed parameters	Number of steps	Energy (a.u.)	Imaginary frequencies Number	Imaginary frequencies Lowest (*i)
Start			(0)	−764.195 637	14	−439
1	Normal	$\omega < 100\ \text{cm}^{-1}$	288	−764.257 355	5	−111
2	Redundant	Torsions	42/crashed	n/a	n/a	n/a
3	Internal	Torsion, bond angles	21	−764.215 254	10	−463
4	Internal	Torsions	6/crashed	n/a	n/a	n/a
5	Internal	Torsions, bond angles except H–O–H	32	−764.225 050	9	−291

As follows from the results presented above, weakly bonded complexes are difficult to optimize by all minimization algorithms, due to the shallow, nonquadratic interaction potential. Because of its stability and speed, the normal mode-based optimization appears to be a better alternative to the internal coordinates in these cases. From our point of view, the biggest advantage of the normal mode optimization is that the coordinates do not have to be defined artificially and the lower-frequency modes are separated out naturally. This enables a reasonable compromise to be implemented between a fully relaxed structure, which is desirable for vibrational spectra calculation in the harmonic approximation, and for particular conformation resembling a natural target structure. Supposedly, the procedure also can be extended for anharmonic potentials.

One would naively think that the normal mode computation requires an additional estimation of the second derivative matrix, which would lead to a dramatic increase of the computational time. However, for the examples we compared, very approximate methods (molecular mechanics, semiempirical molecular orbital methods, etc.) provided a usable first guess for the normal modes. Thus, the initial Hessian estimation does not significantly complicate practical computations. Supposedly, the normal mode spatial movement is primarily determined by the geometrical arrangement of atoms and is restricted by the number of degrees of freedom of the molecule, and thus is less sensitive to inaccuracies in the force field.

In the current implementation, we used the usual Hessian update procedure based on the gradients. Obviously, the Hessian can also be calculated for each geometry along the optimization path. This is not practical for most applications, due to the enormous computational costs of the calculation of second derivatives. Note that computation of the first energy derivatives (gradient) is computationally cheaper than for bare energies, because it does not require SCF iterations.[33] However, the explicit Hessian evaluation may be desirable for special cases, such as small systems or molecular clusters with complicated interactions that significantly change during the geometry optimization.

Finally, it should be noted that the restricted normal mode optimization often cannot be used at all, particularly in all cases when exact valence coordinates are desired, and these must be fixed explicitly. Thus, the normal mode method should be considered rather as a complementary tool to the internal valence coordinate based optimizations. Fortunately, as shown above, both the normal mode and torsional constraints provide in many cases similar results, i.e., fixation of the geometry parameters can be achieved by controlling the vibrational normal modes.

V. CONCLUSIONS

The normal mode-based quantum chemical optimization of molecular geometry provided smooth convergence for all systems studied. For energy minimization of fully relaxed covalent structures its speed tended to be between that obtained with the redundant/internal coordinate method and optimization based on Cartesian coordinates. However, for weakly bonded complexes, especially those with imposed arbitrary constraints on the geometry, the normal mode method was found to be the fastest and most reliable. Its computer implementation is simple and enables a natural separation of the low- and high-frequency molecular movements.

ACKNOWLEDGMENTS

[1] H. B. Schlegel, in *Modern Electronic Structure Theory*, edited by D. R. Yarkony (World Scientific, Singapore, 1995), pp. 459–500.
[2] W. H. Press, S. A. Teukolsky, W. T. Vetterling, and B. P. Flannery, *Numerical Recipes* (Cambridge University Press, Cambridge, 1992).
[3] R. Fletcher and C. M. Reeves, Comput. J. (UK) **7**, 149 (1964).
[4] P. Pulay, Chem. Phys. Lett. **73**, 393 (1980).
[5] P. Pulay, J. Comput. Chem. **3**, 556 (1982).
[6] R. Fletcher and M. J. D. Powell, Comput. J. (UK) **6**, 163 (1963); W. Davidon, Argonne National Lab. Report ANL-5900.
[7] C. G. Broyden, J. Inst. Math. Appl. **6**, 76 (1970); R. Fletcher, Comput. J. (UK) **13**, 317 (1970); D. Goldfarb, Math. Comput. **24**, 23 (1970); D. F. Shanno, *ibid.* **24**, 647 (1970).
[8] R. Fletcher, *Practical Methods of Optimization* (Wiley, Chichester, 1981).
[9] A. Banerjee, N. Adams, J. Simons, and R. Shepard, J. Phys. Chem. **89**, 52 (1985).
[10] J. Simons and J. Nichols, Int. J. Quantum Chem., Quantum Chem. Symp. **24**, 263 (1990).
[11] J. Baker and W. J. Hehre, J. Comput. Chem. **12**, 606 (1991).
[12] H. B. Schlegel, Int. J. Quantum Chem., Quantum Chem. Symp. **26**, 243 (1992).
[13] J. Baker, J. Comput. Chem. **14**, 1085 (1993).
[14] P. Pulay, G. Fogarasi, F. Pang, and J. E. Boggs, J. Am. Chem. Soc. **101**, 2550 (1979).
[15] P. Pulay and G. Fogarasi, J. Chem. Phys. **96**, 2856 (1992).
[16] M. J. Frisch, G. W. Trucks, H. B. Schlegel *et al.*, GAUSSIAN 98 (Revision A.7), Gaussian, Inc., Pittsburgh, PA, 1998.
[17] B. Paizs, J. Baker, S. Suhai, and P. Pulay, J. Chem. Phys. **113**, 6566 (2000).
[18] P. Bouř and T. A. Keiderling, J. Am. Chem. Soc. **114**, 9100 (1992).
[19] R. A. G. D. Silva, J. Kubelka, P. Bouř, S. M. Decatur, and T. A. Keiderling, Proc. Natl. Acad. Sci. U.S.A. **97**(15), 8318 (2000).
[20] J. Baker, J. Comput. Chem. **8**, 563 (1987).
[21] J. Baker, J. Comput. Chem. **7**, 385 (1986).
[22] Ch. J. Cerjan and W. H. Miller, J. Chem. Phys. **75**, 2800 (1981).
[23] C. Peng, P. Y. Ayala, H. B. Schlegel, and M. J. Frisch, J. Comput. Chem. **17**, 49 (1996).
[24] D. Papoušek and M. R. Aliev, *Molecular Vibration-Rotational Spectra* (Academia, Prague, 1982).
[25] H. B. Schlegel, J. Comput. Chem. **3**, 214 (1982).
[26] R. V. Pappu, R. K. Hart, and J. W. Ponder, J. Phys. Chem. B **102**, 9725 (1998).
[27] A. D. Acosta, J. Baker, W. Cordes, and P. Pulay, J. Phys. Chem. A **105**, 238 (2001).
[28] A. Becke, Phys. Rev. A **38**, 3098 (1988).
[29] J. P. Perdew and Y. Wang, Phys. Rev. B **45**, 13244 (1992).
[30] Z. Huang, L. Wang, and Timothy A. Keiderling, in *Spectroscopy of Biological Molecules*, edited by J. C. Merlin (Kluwer Academic, Dordrecht, 1995), pp. 321–322.
[31] T. P. Lybrand, I. Ghosh, and J. A. McCammon, J. Am. Chem. Soc. **107**, 7793 (1985).
[32] W. D. Cornell, P. Cieplak, C. I. Bayly *et al.*, J. Am. Chem. Soc. **117**, 5179 (1995).
[33] J. A. Pople, R. Krishnan, H. B. Schlegel, and J. S. Binkley, Int. J. Quantum Chem., Quantum Chem. Symp. **13**, 225 (1979).